

LA-11726-MS

UC-700 and UC-705
Issued: March 1990

LA--11726-MS

DE90 007154

*Method of Obtaining SESAME
Equations of State for Porous Materials:
Application to Garnet Sand*

*J. C. Boettger
S. P. Lyon*



Los Alamos Los Alamos National Laboratory
Los Alamos, New Mexico 87545

MASTER

DISTRIBUTION OF THIS DOCUMENT IS UNLIMITED

METHOD OF OBTAINING SESAME EQUATIONS OF STATE FOR POROUS MATERIALS: APPLICATION TO GARNET SAND

by

J. C. Boettger and S. P. Lyon

ABSTRACT

The computer program GRIZZLY, used to construct equations of state (EOS) for the SESAME library, has been modified to allow porosity to be treated within a simple ramp type model. In this model, given an EOS for a nonporous material, a new SESAME EOS can be constructed for a porous sample of the same material. The new EOS will exhibit ramp behavior for temperatures below the melting point and will be identical to the EOS of the nonporous material for temperatures significantly above the melting point or for densities slightly larger than the equilibrium density of the nonporous material. The new EOS will be thermodynamically self-consistent everywhere.

This new ramp treatment has been used to construct an EOS for garnet sand (SESAME material number 7761) from an existing equation of state for nonporous garnet.

I. INTRODUCTION

One of the major challenges confronting theorists working on the SESAME equation of state (EOS) library is the question of how to treat irreversible phase transitions. Obviously, the only completely realistic way in which such a transition could be handled is by constructing a separate EOS for each phase of a given material. In principal, the user could then switch from one EOS to the other in some thermodynamically self-consistent fashion as the phase boundary was crossed during a calculation. In reality, few (if any) of the library users have programs capable of doing the type of switching described here. Given that limitation, more approximate methods must be used for describing irreversible phase transitions. In this report, we deal with one class of irreversible phase transitions; the transition of a porous material to a nonporous material, either under

compression or upon melting.

The most common approach to describing irreversible phase transitions in a SESAME EOS is to simply ignore the irreversible nature of the transition and use GRIZZLY to construct a single EOS based on experimental Hugoniot data. The primary advantage of this procedure is that it ensures that the phase transition will be correctly described along the principal Hugoniot. There are two major disadvantages to this approach. First, the phase boundary will be approximated as an isochore and will appear at all temperatures. In addition, the forbidden reverse transition will be allowed and will introduce errors into any calculation which includes a release that extends to densities less than the transition density, regardless of the temperature. Although this approach has been used to produce EOS for a number of materials which exhibit irreversible phase transitions, it has not been applied to porous materials.

There are at least two methods for treating the porous \rightarrow nonporous phase transition currently in use at LANL. Perhaps the most commonly used of these approaches is that embodied in the subroutine package HYDSES² (which acts as a multi-purpose interface between the SESAME library and user codes). In this approach, it is assumed that a complete EOS exists for the nonporous material. HYDSES is then used to construct a special path through P vs. ρ space (formed out of two straight lines) which begins at the initial conditions for the porous material and approximates the transition to the nonporous phase. When this "ramp" intersects the nonporous EOS or the melt line, the transition is assumed to be complete and the ramp is no longer used. The major advantage of this approach is that the transition is treated as a truly irreversible process. The disadvantages are 1) an additional layer of software is used in the calculation, 2) the user is required to know in advance the trajectory through phase space up to the transition, and 3) there are limits on what types of processes can be used to drive the porous \rightarrow nonporous phase transition (e.g. this approach could not be applied to an isobaric transition in which the porous material was simply heated up until it melted).

In the second common approach to the porous \rightarrow nonporous transition, the user simply ignores the porous phase and uses an EOS for the nonporous material everywhere. In this case the initial density used is that of the porous material and the initial pressure will therefore be negative. The rationale behind this approach is that the pressures that the porous material can support without collapsing will be sufficiently small in magnitude that replacing them with small negative values will not seriously affect the calculation. Although this approach has the obvious advantage of simplicity, its validity is questionable at best.

In this report, we describe an alternative approach to describing the porous \rightarrow nonporous transition, which has been added to the program GRIZZLY.¹ In this approach, given an EOS for a nonporous material, an EOS for the porous material can be easily constructed. The cold curve (zero temperature isotherm) of the new EOS will have a ramp form for densities ranging between the equilibrium densities of the porous and nonporous materials. At a slightly higher density, where the ramp intersects the nonporous cold curve, the cold curve becomes identical to that of the nonporous material. The other isotherms will also have a ramp behavior for temperatures up to near the melt temperature. Over some reasonably small range of temperatures, centered about the melt temperature, the new EOS will be smoothly transformed into the nonporous EOS. This approach is most closely related to the standard method used to describe irreversible transitions other than the porous \rightarrow nonporous transition, in that the irreversible nature of the phase transition is ignored. However, the phase boundary in this method is formed from an isochore at the transition density and an isotherm at the melting temperature. For larger temperatures and densities, the new EOS becomes identical to the old one.

In the next section, the new ramp technique is presented and discussed. In Section III, this technique is used to generate a SESAME EOS for garnet sand (material number 7761) using an existing EOS for garnet, and the new EOS is analyzed in detail.

II. NEW RAMP METHOD

Most of the EOS in the SESAME library are partitioned into three terms for the pressure P , the internal energy E , and the free energy A :

$$P(\rho, T) = P_s(\rho) + P_n(\rho, T) + P_e(\rho, T) \quad (1)$$

$$E(\rho, T) = E_s(\rho) + E_n(\rho, T) + E_e(\rho, T) \quad (2)$$

$$A(\rho, T) = A_s(\rho) + A_n(\rho, T) + A_e(\rho, T) \quad (3)$$

where ρ is the density and T is the temperature. The subscripts s , n , e denote the contributions due to the static lattice (i.e. frozen nuclei) cold curve (zero temperature isotherm), the nuclear motion, and the thermal electronic excitations. It is thus possible to treat each contribution independently using any desired model. The free energy A can be related to the energy as:

$$A(\rho, T) = E(\rho, T) - T S(\rho, T) \quad (4)$$

where S is the entropy.

In the following discussion, we will assume that a SESAME type EOS, including tables for all of the contributions defined above, already exists for some nonporous material, and that a new SESAME EOS is desired for a porous version of the same material. The porous material is assumed to be well characterized with some known reference density and temperature (ρ_r and T_r) at which $P = 0$. It is further assumed that the P vs. ρ static lattice cold curve can be divided into three distinct regions under compression: 1) A porous region which is linear and has a bulk modulus of B_0 at the $P = 0$ point; 2) A transition (or crush) region which begins when P reaches some crush pressure P_c , is linear, and has an initial bulk modulus of B_c ; and 3) A nonporous region in which the porous EOS is identical to the nonporous EOS. The porous EOS is also assumed to smoothly transform into the nonporous EOS as the temperature passes T_m . Finally, it is assumed that for a given T and ρ , the contributions due to the nuclear motion and thermal elec-

tronic excitations are identical for the porous and nonporous materials.

Based on the preceding discussion, the P vs. ρ static lattice cold curve will be of the form:

$$P_i^p(\rho) = (B_0/\rho_0) (\rho - \rho_0) \quad \rho_r < \rho < \rho_c \quad (5a)$$

$$P_i^p(\rho) = (B_c/\rho_c) (\rho - \rho_c) + P_c \quad \rho_c < \rho < \rho_i \quad (5b)$$

$$P_i^p(\rho) = P_i^{np}(\rho) \quad \rho_i < \rho \quad (5c)$$

where the superscripts np and p indicate nonporous and porous, respectively.

In the program GRIZZLY, the empirical parameters ρ_r , T_r , B_0 , P_c , and B_c are read in as RAMPDR, RAMPTR, RAMPBR, RAMPPC, and RAMPBC. Then, when GRIZZLY executes the RAMP option, ρ_0 is calculated from the requirement that $P(\rho_r, T_r) = 0$, ρ_c is found by setting Eq. 5a equal to P_c , and ρ_i is determined by the intercept of 5b and 5c. The energy and free energy of the static lattice cold curve in the porous and crush regions are then calculated by analytical integration of 5a and 5b, subject to the constraint that the energy at ρ_i should be identical to the energy of the nonporous material. The static lattice cold curve is completed by adding on a Lennard-Jones tail in the expanded region and GRIZZLY requires specification of all of the usual parameters needed to construct that tail (ABAR, ECOH, FACLJ, MODN, and IGRUN).

The ramp behavior of the static lattice cold curve described above would now appear in all of the isotherms for the porous EOS, if the SESAME tables for the nuclear and electronic contributions were left identical to those for the nonporous EOS. However, we want the total EOS to become identical to the nonporous EOS for temperatures slightly larger than T_m . Thus, we must somehow effectively replace the porous cold curve with the nonporous cold curve in a smooth, thermodynamically self-consistent fashion as the temperature is increased. To accomplish this, we have chosen to add corrections ($\Delta A_n(\rho, T)$, $\Delta E_n(\rho, T)$, and $\Delta P_n(\rho, T)$) to the nuclear table which are required to be zero for $T = 0$ and equal to the difference between the nonporous and porous cold curves for temperatures which are significantly larger than T_m . This ensures that both the total EOS and the so-called ionic EOS (the sum of the cold curve and the nuclear EOS) will have

the correct behavior.

We begin by defining an entropy change associated with the transition from the porous phase to the nonporous phase at the melt:

$$\Delta S_n(\rho, T) = -\Delta E_s(\rho) F(T) / T_m \quad (6)$$

where

$$\Delta E_s(\rho) = E_s^{np}(\rho) - E_s^f(\rho) \quad (7)$$

is the difference in energy between the cold curves of the porous and nonporous materials, and

$$F(T) = C \left[\exp\left[\frac{T-T_m}{T_w}\right] + 1 \right]^{-1} \quad (8)$$

$$C = \left\{ \frac{T_w}{T_m} \ln \left[1 + \exp\left[\frac{T_m}{T_w}\right] \right] \right\}^{-1}$$

is a Fermi function (normalized to an integrated value of T_m) which switches from an initial value of C to 0 over a region whose width is roughly T_w centered around T_m . In the limit $T_w \rightarrow 0$, $F(T)$ becomes a step function.

The free energy correction is determined by integrating the entropy correction with respect to T to get:

$$\Delta A_n(\rho, T) = \Delta E_s(\rho) G(T) / T_m \quad (9)$$

with:

$$G(T) = C \left\{ T + T_w \ln \left[\frac{F(T)}{F(0)} \right] \right\} \quad (10)$$

The internal energy correction is then given by Eq. 4 as:

$$\Delta E_n(\rho, T) = \Delta E_s(\rho) [G(T) - T F(T)] / T_m . \quad (11)$$

Similarly, the pressure correction is:

$$\Delta P_n(\rho, T) = \Delta P_s(\rho) [G(T) - T F(T)] / T_m . \quad (12)$$

The temperature dependent functions $F(T)/T_m$, $G(T)/T_m$, and $[G(T) - T F(T)]/T_m$ are shown in Fig. 1 for several values of (T_w/T_m) . Note that the latter two of these functions range from 0 to 1. Thus the corrections to the nuclear curve will effectively replace the porous cold curve with the nonporous cold curve as the temperature exceeds T_m . Since the corrections to the EOS are determined via the entropy using standard thermodynamic relationships, the corrections will be thermodynamically self-consistent everywhere.

In GRIZZLY, the needed parameters T_m and (T_w/T_m) are specified in the input as TMELT and RAMPFF. Once all of the needed input parameters have been read into GRIZZLY, the RAMP command can be executed.

RAMP $i_1 i_2 i_3 i_4 i_5 /$

where i_1 , i_2 , and i_3 denote the labels for the nonporous 304, 305, and 306 tables. After executing RAMP, i_1 , i_2 , i_4 , and i_5 will be the labels of the 304, 305, 306, and 301 tables for the SESAME EOS of the porous material.

III. GARNET SAND (7761)

Garnet sand provides a convenient test case for the ramp model described in the previous section for several reasons. First, garnet sand is of interest to several users of the SESAME library. In addition, a SESAME EOS for bulk garnet already exists in the SESAME library (material number 7760). Finally, unlike most porous materials (eg. foams), garnet sand is a reasonably well characterized material in the sense that its porosity should not vary greatly from sample to sample. This last property is important for any porous material whose EOS is to be included in the library. For materials such as polymer foams which exhibit a wide range of porosities, it would

be more practical to store only the EOS for the nonporous material in the library and then produce a special EOS for any desired porosity without including it in the library.

The new EOS for garnet sand (material number 7761) is based on an early version of the garnet EOS in the library (7760) prior to the inclusion of Maxwell constructions.³ The reference density for garnet sand (2.4 gm/cc) is roughly 60% of that for bulk garnet (4.05 gm/cc).³ The values of the various parameters required for construction of the expanded cold curve are consistent with those used for constructing 7760; ABAR = 23.677, ECOHKC = 140 kcal/mole, FACLJ = 0.235, MODN = CHARTJD, IGRUN = 1, GAMREF = 1.0, and DEBKEL = 1000 K.³ The value of B_0 (RAMPBR = 1.0 Mbar) has been assumed to be somewhat smaller than the reference bulk modulus used in 7760.³ The crush pressure (RAMPPC = 0.003 Mbar) used here is based on the known range of crush pressures observed for other rocks and minerals.⁵ The bulk modulus of the cold curve at the crush pressure has been assigned the value RAMPBC = 0.01 Mbar. The melt temperature used (TMELT = 1800) was taken from 7760,³ while the ratio T_w/T_m has been arbitrarily set to 0.1 (= RAMPFF).

The zero temperature P vs. ρ isotherms of bulk garnet and garnet sand (7761) are compared in Figure 2. Note that the 0 K isotherm for 7761 merges with that of bulk garnet for densities greater than about 4.1 gm/cc. In Figure 3, several P vs. ρ isotherms for garnet sand are displayed. As the temperature is increased to near T_m (1800 K), the isotherms begin to cross the 0 K isotherm. Once T has achieved roughly $1.5 T_m$, the isotherms for garnet sand are indistinguishable from those for bulk garnet. The fact that the P vs. ρ isotherms cross is to be expected since the disappearance of the porosity upon melting will result in a reduction of pressure at fixed volume. This form for the isotherms of garnet sand also ensures the correct behavior of the EOS for isobaric heating from ambient conditions, i.e. an initial expansion of the sand, followed by a volume collapse during the melt transition.

Although crossing P vs. ρ isotherms are desirable for garnet sand, it is crucial that the E vs. ρ

isotherms do not cross, since that would imply a negative specific heat at constant volume (C_v). Figure 4 shows several E vs. ρ isotherms for 7761. As desired, none of the energy isotherms cross. A more stringent test is provided by plotting C_v vs. T for various values of ρ in the ramp region (see Figure 5). The specific heat is positive everywhere as required and exhibits a substantial peak near T_m which corresponds to the porous \rightarrow nonporous phase transition at the melt. (Although this is the correct qualitative form for C_v , there is no assurance that the structure at T_m is quantitatively correct.) The fact that the E vs. ρ of 7761 do not cross also ensures that for a given value of ρ , E is a single valued function of T . Hence, there should be no difficulty involved in converting the SESAME tables into the so-called inverted tables with E replacing T as an independent variable.

Having demonstrated that there is no pathological behavior in the new SESAME EOS for garnet sand, we should next assess the impact of the spurious reversability of the porous \rightarrow nonporous transition. The most common use of the SESAME library is in hydrodynamic calculations under shock conditions. Thus, the most important process to be considered is shock loading along the principal Hugoniot followed by an adiabatic release. In Figure 6, the principal Hugoniot for garnet sand is shown in P vs. ρ space together with the release adiabats associated with selected shock pressures ranging up to 350 kbar. The release adiabats in Fig. 6 are truncated at $P = 0.0$, since the garnet sand will not be able to support any substantial tension. From Fig. 6, it is clear that for shock pressures up to about 250 kbar, the release adiabat will extend into the ramp region and that portion of the adiabat will be incorrect. For shock pressures greater than about 250 kbar, the release adiabat will not enter the ramp region and should be reliable down to the $P = 0.0$ point.

Potential users of this new EOS for garnet sand should keep in mind the limitations described above when using 7761. In principal, the difficulties associated with the irreversibility of the porous \rightarrow nonporous transition could be avoided by combined use of 7761 (garnet sand) and 7760

(garnet). Since the two EOS are identical for densities greater than about 4.1 gm/cc or for temperatures greater than about 3000 K, one could use 7761 to describe shock loading and then use 7760 to describe the subsequent adiabatic release.

REFERENCES

1. Joseph Abdallah, Jr., "User's Manual for GRIZZLY," Los Alamos National Laboratory report LA-10244-M (September 1984).
2. Joseph Abdallah, Jr., G. I. Kerley, B. I. Bennett, J. D. Johnson, R. C. Albers, and W. F. Huebner, "HYDSES: A Subroutine Package for Using Sesame in Hydrodynamic Codes," Los Alamos National Laboratory Report LA-8209 (June 1980).
3. J. D. Johnson, Los Alamos National Laboratory, personal communication, September 1989.

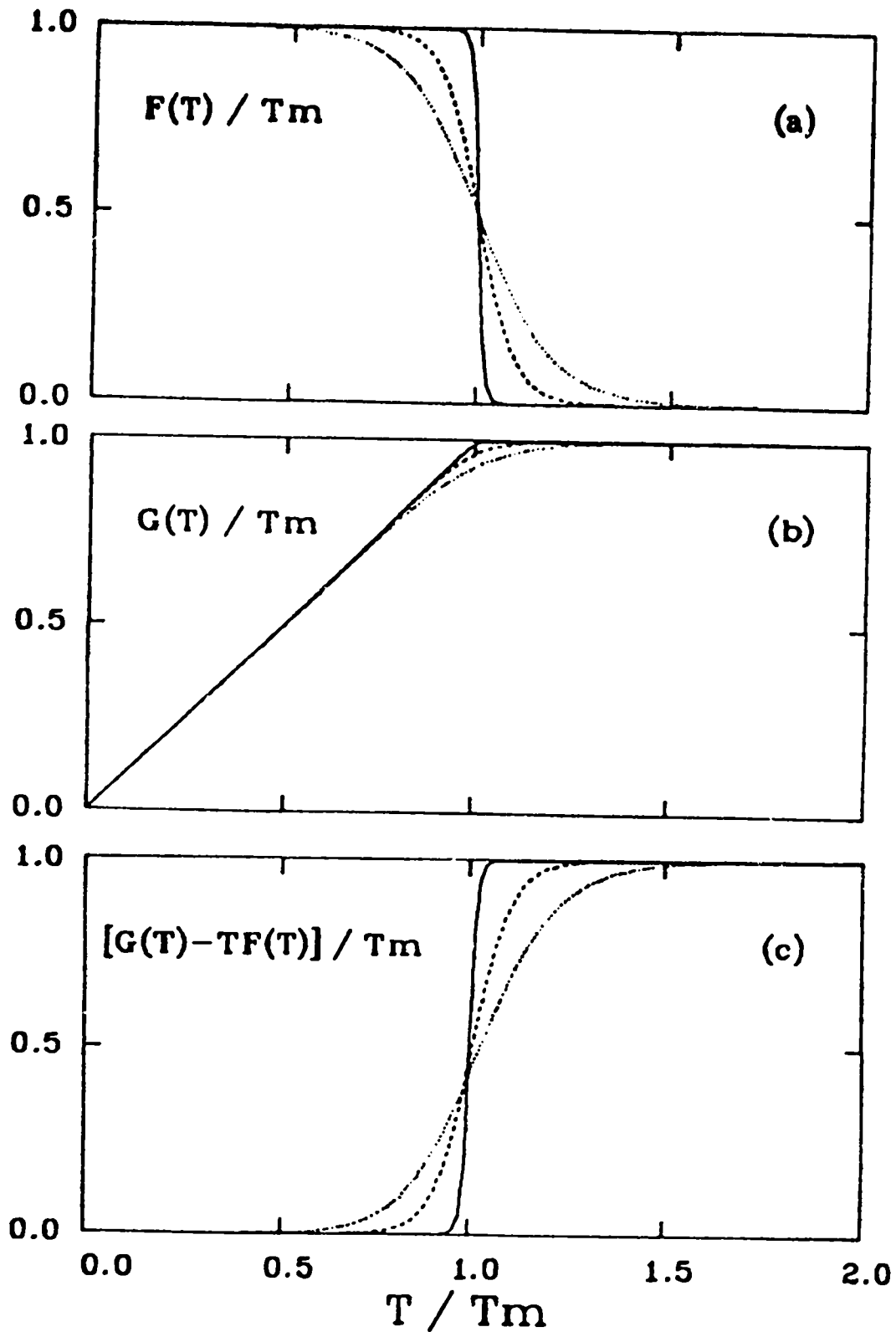


Fig. 1. The temperature dependent functions $F(T)/T_m$ (a), $G(T)/T_m$ (b), and $[G(T)-T F(T)]/T_m$ (c) are shown for $(T_w/T_m)=0.01$ (solid line), 0.05 (dashed line), and 0.10 (dotted line).

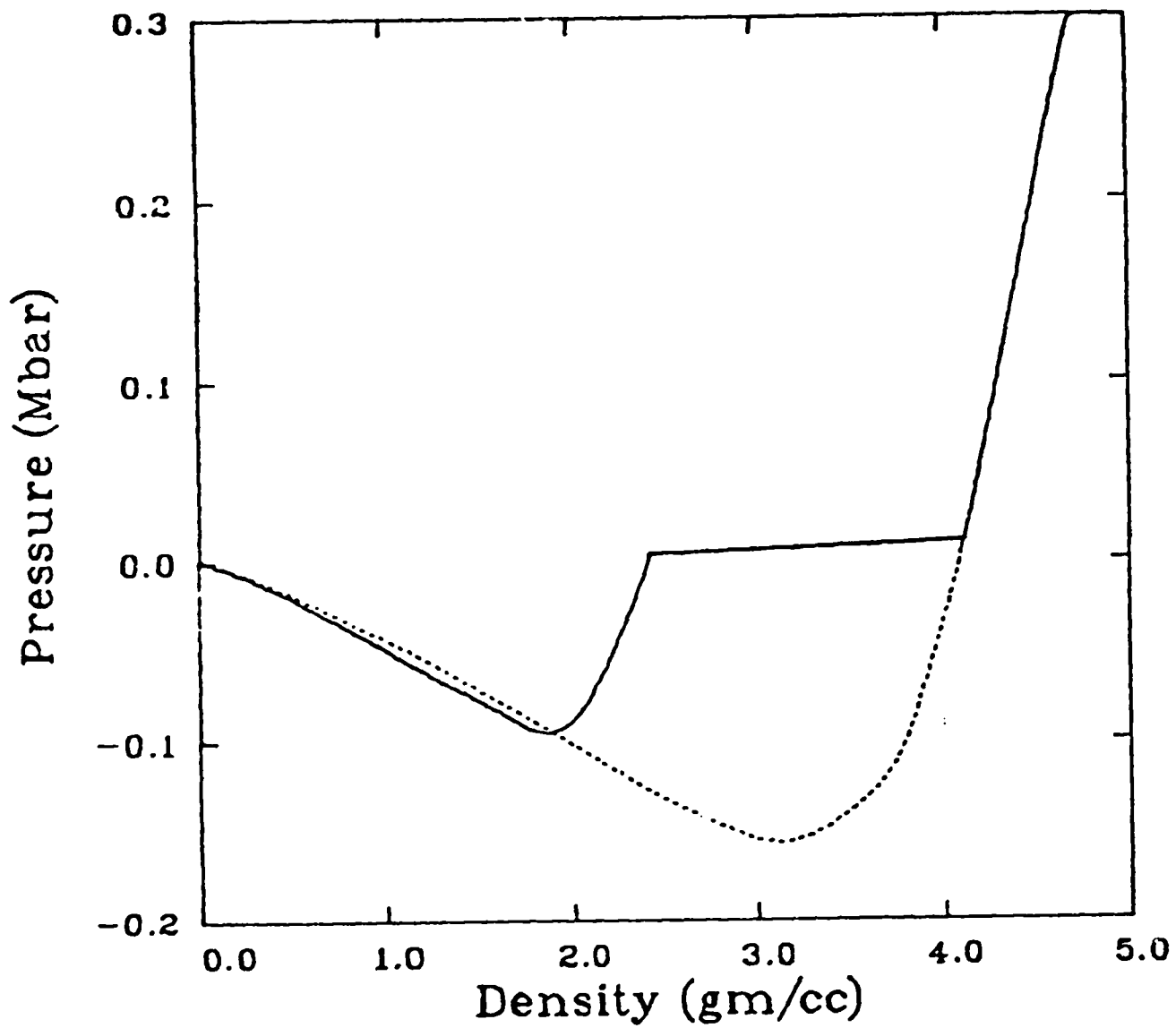


Fig. 2. Calculated cold curve for garnet sand (solid line) compared with that of bulk garnet (dashed line).

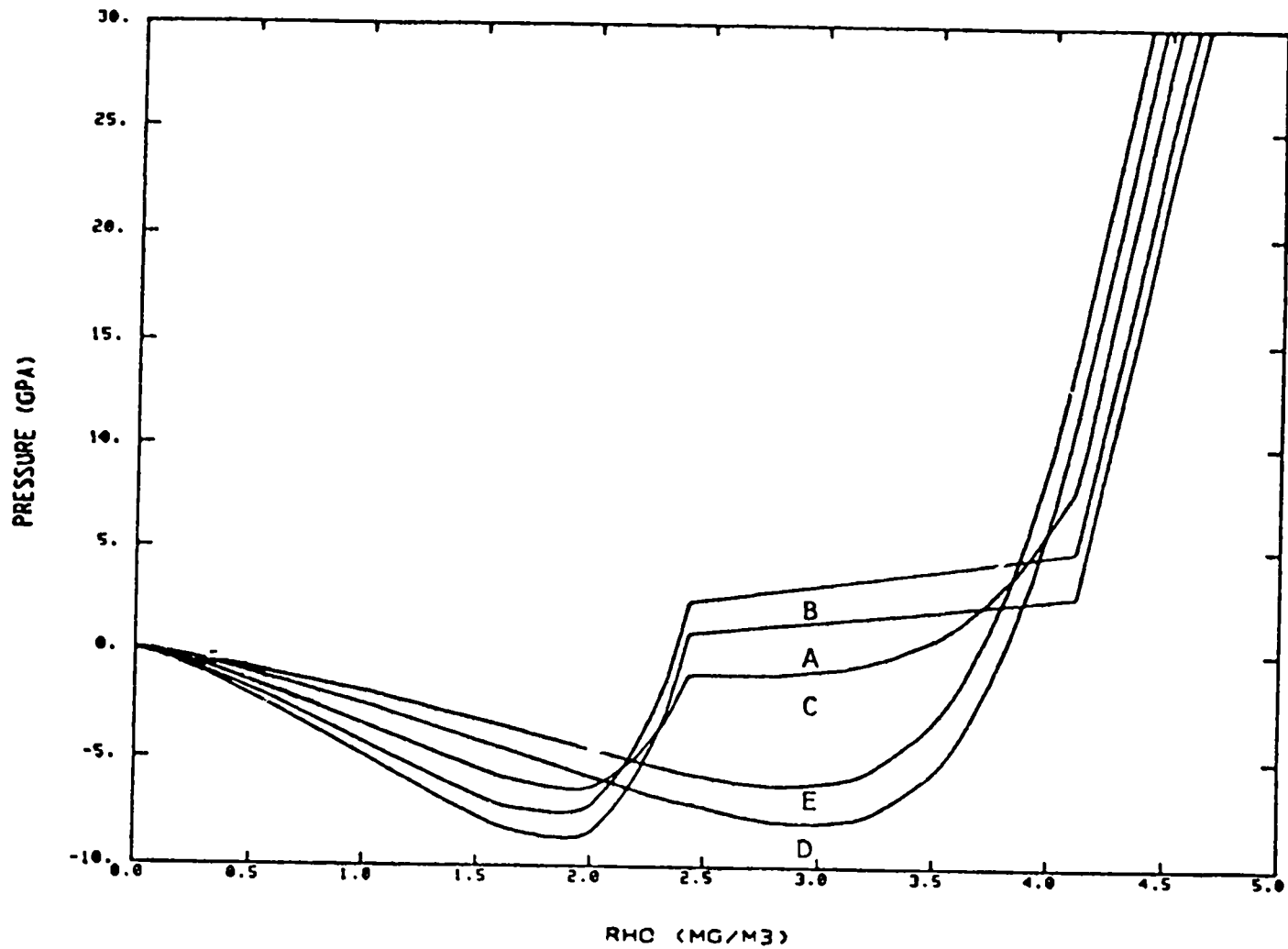


Fig. 3. Calculated P vs. density isotherms for garnet sand for $T/T_m =$ (A) 0.0, (B) 0.5, (C) 1.0, (D) 1.5, and (E) 2.0.

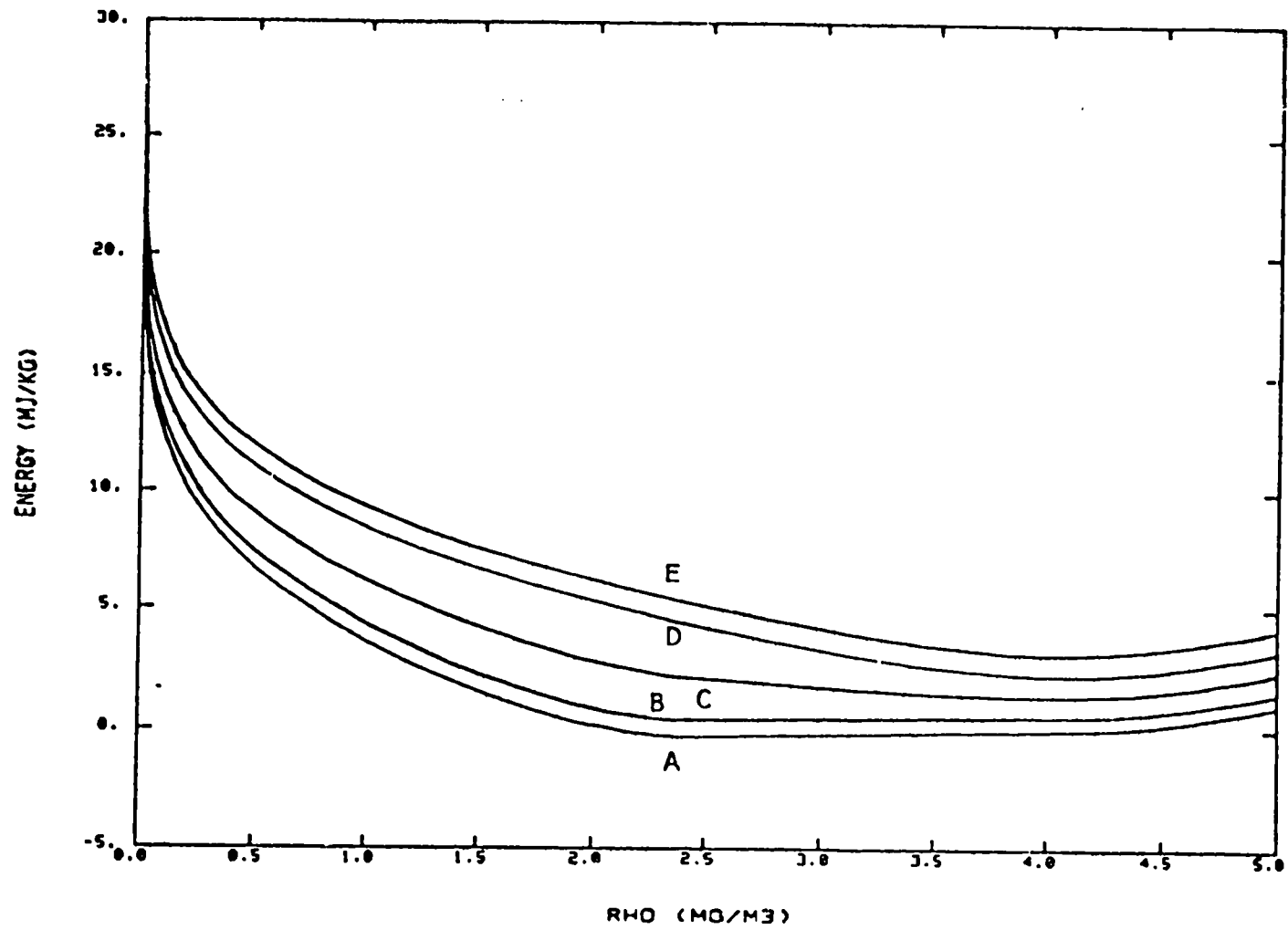


Fig. 4. Same as Figure 3 except for E vs. density isotherms.

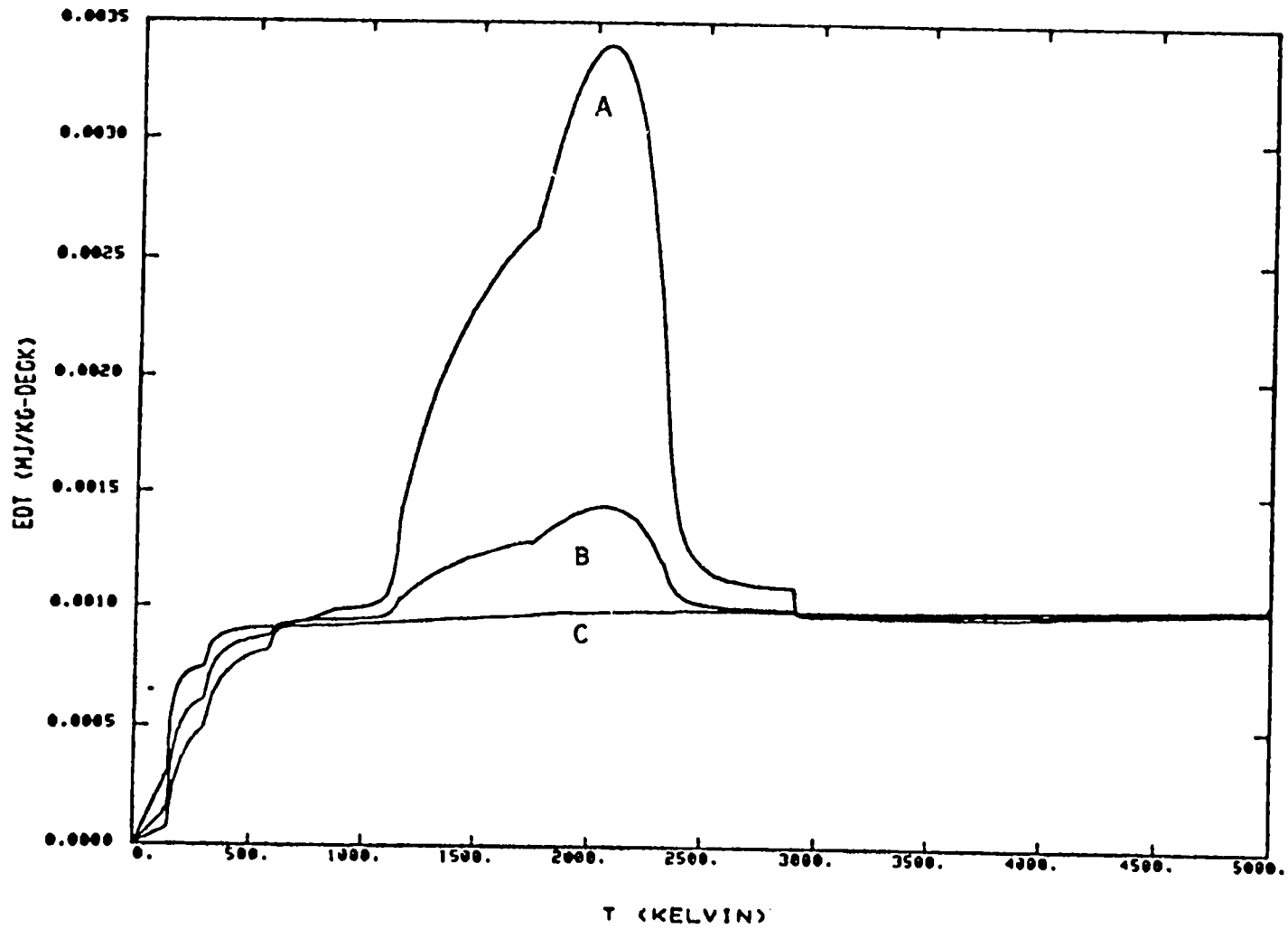


Fig. 5. The specific heat at constant volume, C_V vs. T , for densities of (A) 2.5 gm/cc, (B) 3.5 gm/cc, and (C) 4.5 gm/cc.

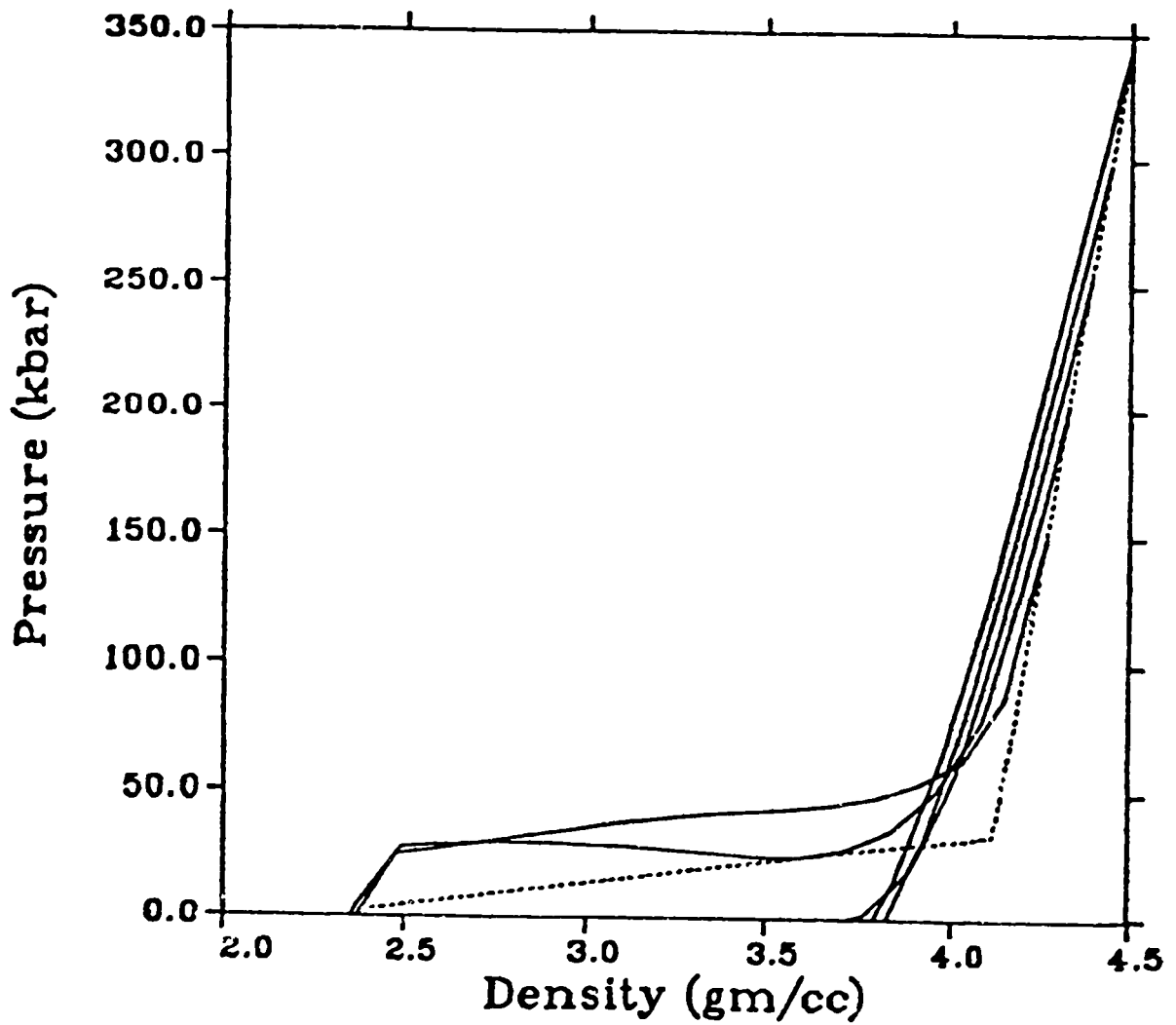


Fig. 6. Principal Hugoniot (dashed line) for garnet sand and release adiabats (solid lines) with initial pressures of 150 kbar, 200 kbar, 250 kbar, 300 kbar and 350 kbar.